Available online at www.sciencedirect.com

ScienceDirect

Mendeleev Commun., 2023, **33**, 556–558

Mendeleev Communications

Effect of hyaluronic acid encapsulation in a silica hydrogel matrix on drug penetration through the skin

Ekaterina S. Dolinina* and Elena V. Parfenyuk

G. A. Krestov Institute of Solution Chemistry, Russian Academy of Sciences, 153045 Ivanovo, Russian Federation. Fax: +7 493 233 6237; e-mail: terrakott37@mail.ru

DOI: 10.1016/j.mencom.2023.06.037

It has been found that the encapsulation of high molecular weight hyaluronic acid in a biologically relevant silica hydrogel matrix provides its accelerated penetration into the skin compared to free acid. The developed hybrid hydrogels, in which high molecular weight hyaluronic acid retains its pronounced anti-inflammatory properties and strong hydrating effect, can become the basis for new, more effective soft formlations for the treatment of inflammatory skin diseases, as well as for products used in the beauty industry. It has been shown that the penetration of hyaluronic acid from the hybrid hydrogels depends on the conditions of their synthesis, the average molecular weight and the loading of the acid.

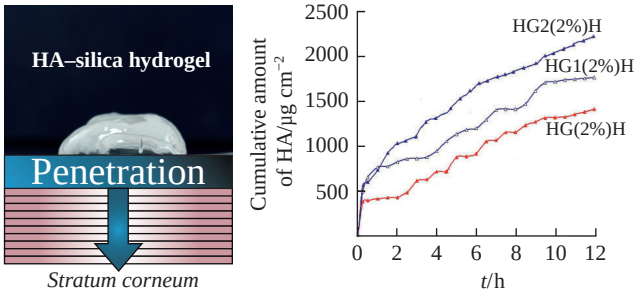

Keywords: silica, hyaluronic acid, hybrid hydrogel, skin penetration rate, apparent permeability coefficient.

Polymer hydrogels are often proposed as new materials for medicine and cosmetics.[1–5] Hyaluronic acid (HA) hydrogels and materials based on them are of particular interest, since they are already used clinically or are proposed for the treatment of various inflammatory diseases.[6,7] HA is a favorite among the ingredients of beauty products.[8,9]

The most important property of soft drug formulations for topical application to the skin is their ability to penetrate into the deeper layers of the skin, where they are expected to act. This ability depends on the molecular weight of the drug. Published studies have shown that low to medium average molecular weight HA (1–300 kDa) penetrates well into or through human or animal skin, whereas high molecular weight HA (1000–1500 kDa) does not.[10,11] It should be noted that high molecular weight HA has more pronounced anti-inflammatory properties compared to low molecular weight HA.[12,13] Therefore, various strategies have been proposed to improve the penetration of high molecular weight HA. A number of studies have shown that encapsulation of the acid in materials of different nature can increase its penetration through the skin. For example, Kasetvatin *et al.*[14] encapsulated a high molecular weight acid in liposomes, resulting in an improvement in skin permeability to acid by about 12%. Chen *et al.*[15] showed that the encapsulation of HA in a lipid shell formed by the SPACE peptide increased the permeability of porcine and human skin to HA by several times.

In the present work, we investigated the percutaneous penetration of HA encapsulated in silica hydrogel matrices. Sol–gel synthesis of HA–silica hybrid hydrogel materials and study of the influence of synthesis conditions (the concentration of HCl as a catalyst for the formation of silica sol and the amount of added HA) and the average molecular weight of the acid on the morphology of the resulting hydrogels, their deformation properties under shear, compression and tension, as well as the kinetics of release into buffer solutions simulating biological media have been described in our previous work.[16] The present study is devoted to the investigation of the effects of the above factors on the penetration characteristics of HA through the chicken skin. Although bird skin is thinner and has certain differences from human skin,[17] chicken skin is often used as a biological model for the transdermal transport of various substances.[18–20] In this work, chicken skin was used as a model for studying the penetration of HA into the deeper layers of the skin.

The investigated HA–silica hydrogels were designated as HGX(Y)Z, where X = (1 or 2) refers to hydrogels synthesized using 0.030 M or 0.125 M HCl, respectively, Y = (1% or 2%) refers to the concentration of HA in the hydrogels and Z = (L, M or H) refers to HA with low (20–50 kDa), medium (50–100 kDa) or high (1000–1500 kDa) molecular weight, respectively. The data obtained were compared with those of pure HA hydrogels HG(Y)Z. *Ex vivo* experimental methods and quantification of HA in receptor medium (acetate buffer, pH 5.5) are described in detail in Online Supplementary Materials.

As an example, Figure 1 shows the cumulative kinetic profiles of penetration of low and high molecular weight HA through a unit area of skin surface from hydrogels of pure acid and acid encapsulated in silica hydrogel matrices.

As can be seen from the figure, there are small burst effects in the dependences at 0.25–0.5 h. In addition to lag effects, burst effects were observed quite often in studies of transdermal transport of various drugs.[21–23] After the burst effect, the cumulative profiles are well described by a zero-order kinetic model (R^2 = 0.96–0.98):

$$\left(Q_t/A\right) = Q_0 + k_0 t, \quad (1)$$

where A (cm^2) is the skin surface area, Q_0 and Q_t (μg cm^{-2}) are the initial amount of HA in the receptor medium and the cumulative amount of HA that has penetrated in time t (h) through a unit area

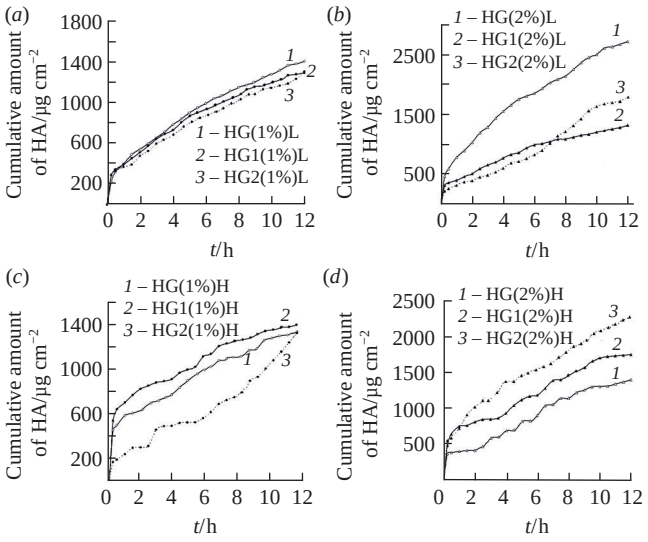

Figure 1 Experimental cumulative kinetic profiles of percutaneous penetration of HA from hydrogels containing (*a*),(*b*) low molecular weight and (*c*),(*d*) high molecular weight acids. Conditions: temperature 32 °C and acetate buffer (pH 5.5) as receptor medium.

of the skin, respectively, and k_0 is the zero-order rate constant. The penetration rate or steady-state flux J (μg cm^{-2} h^{-1}) of HA through the skin barrier was calculated as the slope of the cumulative profiles and was equal to k_0:

$$J = \frac{\mathrm{d}\left(Q_t/A\right)}{\mathrm{d}t} = k_0. \quad (2)$$

The apparent skin membrane permeability coefficient P (g cm^{-2} h^{-1}) was calculated as

$$P = J/C_0, \quad (3)$$

where C_0 (μg per g of hydrogel) is the amount of HA in the hydrogel sample.

Table 1 shows the values of the above characteristics, as well as the experimental values of the amount of HA that penetrated into the receptor medium in 12 h per unit area, Q_{12} (exp). It also shows penetration characteristics for 1% and 2% hydrogels of pure HA. The analysis of the data obtained made it possible to identify the key features of the process.

Table 1 HA penetration characteristics from pure hydrogels and HA–silica hybrid hydrogels.

Hydrogel	J^a/μg cm^{-2} h^{-1}	$P \times 10^3$/g cm^{-2} h^{-1}	Q_{12} (exp)/μg cm^{-2}
HG(1%)L	101 ± 5	9.7	1404
HG1(1%)L	89 ± 3	9.2	1289
HG2(1%)L	97 ± 4	9.5	1295
HG(2%)L	195 ± 19	9.6	2725
HG1(2%)L	92 ± 4	4.8	1323
HG2(2%)L	142 ± 11	7.2	1755
HG(1%)M	89 ± 6	8.7	1143
HG1(1%)M	56 ± 3	5.7	905
HG2(1%)M	76 ± 3	8.1	1003
HG(2%)M	98 ± 3	4.7	1289
HG1(2%)M	77 ± 2	4.2	1025
HG2(2%)M	80 ± 2	4.2	1232
HG(1%)H	84 ± 5	7.9	1325
HG1(1%)H	71 ± 5	7.1	1383
HG2(1%)H	89 ± 3	7.6	1318
HG(2%)H	98 ± 4	4.6	1398
HG1(2%)H	110 ± 3	5.7	1749
HG2(2%)H	118 ± 5	6.6	2147

[a] Data are presented as an average value ± SD (n = 3).

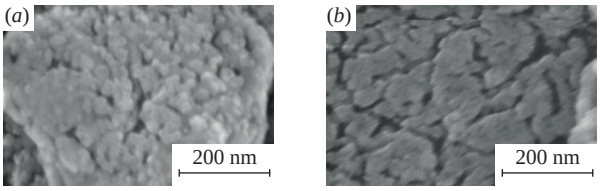

Figure 2 SEM images of (*a*) HG1(2%)M and (*b*) HG2(2%)M.

The data presented in Table 1 show that the penetration characteristics of HA increase with increasing concentration of HCl used as a catalyst for the formation of a silica sol, regardless of the average molecular weight of the acid and its loading. This behavior may be related to the different morphology and particle size of the hybrid materials, as can be clearly seen from the scanning electron microscope (SEM) images in Figure 2, which show SEM images of dried HG1(2%)M and HG2(2%)M as an example. As can be seen from the images, the structure of dried HG1(2%)M consists of strongly condensed aggregates of spherical particles, whereas the structure of dried HG2(2%)M has a layered morphology of smaller particles.

These differences may be associated with different gelation rates during the formation of hybrid hydrogels. Although the gelation process in the presence of HA occurs within a few minutes, the gelation time of hydrogels prepared using 0.125 M HCl increased by up to 2.5 times compared to the gelation time of hydrogels prepared using 0.030 M HCl, for example, 18 min for HG2(2%)M and 7 min for HG1(2%)M. Apparently, the layered matrix is less strong, which leads to its faster degradation and, as a result, to an acceleration of the penetration of HA through the skin barrier, as well as to an increase in the permeability coefficient and the amount of HA that penetrated the skin barrier during the experiment. The fact that hydrogel matrices break down during penetration is evidenced by bands in the electronic absorption spectra of the receptor medium associated with light scattering by silica particles (Figure S1, see Online Supplementary Materials). The faster penetration process may also be facilitated by the decreased particle size of the silica matrix. The indicated effect of particle size on the rate and depth of drug penetration has been noted in a number of studies.[24–26]

According to equation (3), the apparent permeability coefficient of the skin for HA decreases with increasing loading of HA in hybrid hydrogels, whereas the permeation rate of HA increases. The permeation rate is directly proportional to the concentration gradient of HA in the donor and receptor chambers, which is the higher, the higher the acid loading in hydrogels.

Comparison of the permeation characteristics for pure HA hydrogels and hybrid hydrogels presented in Table 1 shows that the encapsulation of low and medium molecular weight acid in silica hydrogel matrices retards its penetration through the skin. The same is observed for hybrid hydrogels containing 1% high molecular weight HA. However, the penetration process is significantly accelerated and skin permeability is increased for hybrid hydrogels containing 2% high molecular weight HA.

There are several reasons for this behavior. In contrast to low and medium molecular weight HA, high molecular weight HA in solution are characterized by the effect of entanglement of polymer chains, which increases with increasing acid concentration.[27–29] The entanglement effect leads to a decrease in the binding sites of HA to the silica matrix and a weakening of the interaction between them, which can lead to an improvement in the penetration characteristics of HA from HG1(2%)H and HG2(2%)H. Another reason could be the hydration state of HA

in the mentioned hydrogels. As shown in published papers, water is one of the main enhancers of skin permeability, especially for hydrophilic substances.[30–32] High molecular weight HA are capable of retaining a huge amount of water, much more than low and medium molecular weight acids. Also, apparently, the encapsulation of high molecular weight HA in a highly hydrophilic silica matrix significantly increases the hydration potential of the system. Spreading such hydrogels on the skin contributes to its significant hydration, which leads to an increase in the penetration characteristics of HA from HG1(2%)H and HG2(2%)H.

The established fact of increased penetration into the skin of high molecular weight HA encapsulated in a silica hydrogel matrix, compared to free acid, is of practical importance. Since high molecular weight HA has anti-inflammatory properties and a pronounced hydrating effect, hybrid hydrogels HG1(2%)H and HG2(2%)H can become the basis for the development of new, more effective soft formulations for the treatment of inflammatory skin diseases (acne, dermatitis, psoriasis, *etc.*), as well as cosmetic compositions.

The authors are grateful to the Upper Volga Regional Center for Physicochemical Research for the opportunity to study the obtained materials by the SEM method.

Online Supplementary Materials

Supplementary data associated with this article can be found in the online version at doi: 10.1016/j.mencom.2023.06.037.

References

1 M. Yu. Gorshkova, L. V. Vanchugova, I. F. Volkova, I. V. Obydennova, I. L. Valuev and L. I. Valuev, *Mendeleev Commun.*, 2022, **32**, 189.
2 S. H. Aswathy, U. Narendrakumar and I. Manjubala, *Heliyon*, 2020, **6**, e03719.
3 I. I. Preobrazhenskiy and V. I. Putlyaev, *Mendeleev Commun.*, 2023, **33**, 83.
4 N. N. Sigaeva, R. R. Vil'danova, A. V. Sultanbaev and S. P. Ivanov, *Colloid J.*, 2020, **82**, 311 (*Kolloidn. Zh.*, 2020, **82**, 363).
5 I. I. Preobrazhenskii and V. I. Putlyaev, *Russ. J. Appl. Chem.*, 2022, **95**, 775 (*Zh. Prikl. Khim.*, 2022, **95**, 685).
6 A. Marinho, C. Nunes and S. Reis, *Biomolecules*, 2021, **11**, 1518.
7 L. H. Chen, J. F. Xue, Z. Y. Zheng, M. Shuhaidi, H. E. Thu and Z. Hussain, *Int. J. Biol. Macromol.*, 2018, **116**, 572.
8 S. N. A. Bukhari, N. L. Roswandi, M. Waqas, H. Habib, F. Hussain, S. Khan, M. Sohail, N. A. Ramli, H. E. Thu and Z. Hussain, *Int. J. Biol. Macromol.*, 2018, **120**, 1682.
9 A. La Gatta, R. Salzillo, C. Catalano, A. D'Agostino, A. V. A. Pirozzi, M. De Rosa and C. Schiraldi, *PLoS One*, 2019, **14**, e0218287.
10 M. Essendoubi, C. Gobinet, R. Reynaud, J. F. Angiboust, M. Manfait and O. Piot, *Skin Res. Technol.*, 2016, **22**, 55.
11 E. J. Shin, J. W. Park, J. W. Choi, J. Y. Seo and Y. I. Park, *Journal of the Society of Cosmetic Scientists of Korea*, 2016, **42**, 235.
12 M. F. P. Graça, S. P. Miguel, C. S. D. Cabral and I. J. Correia, *Carbohydr. Polym.*, 2020, **241**, 116364.
13 R. Altman, A. Bedi, A. Manjoo, F. Niazi, P. Shaw and P. Mease, *Cartilage*, 2019, **10**, 43.
14 C. Kasetvatin, S. Rujivipat and W. Tiyaboonchai, *Colloids Surf., B*, 2015, **135**, 458.
15 M. Chen, V. Gupta, A. C. Anselmo, J. A. Muraski and S. Mitragotri, *J. Controlled Release*, 2014, **173**, 67.
16 E. Parfenyuk and E. Dolinina, *Pharmaceutics*, 2023, **15**, 77.
17 L. Souci and C. Denesvre, *Vet. Res.*, 2021, **52**, 21.
18 T. S. Nipun and S. M. Ashraful Islam, *Saudi Pharm. J.*, 2014, **22**, 343.
19 A. J. Sami, M. Khalid, T. Jamil, S. Aftab, S. A. Mangat, A. R. Shakoori and S. Iqbal, *Int. J. Biol. Macromol.*, 2018, **108**, 324.
20 M. I. Reza, D. Goel, R. K. Gupta and M. H. Warsi, *Int. J. Pharm. Pharm. Sci.*, 2018, **10** (3), 162.
21 M. Aqil, Y. Sultana, A. Ali, K. Dubey, A. K. Najmi and K. K. Pillai, *Drug Delivery*, 2004, **11**, 27.
22 J. Shokri, Sh. Azarmi, Z. Fasihi, S. Hallaj-Nezhadi, A. Nokhodchi and Y. Javadzadeh, *Res. Pharm. Sci.*, 2012, **7**, 225.
23 C. G. M. Gennari, F. Selmin, S. Franzè, U. M. Musazzi, G. M. G. Quaroni, A. Casiraghi and F. Cilurzo, *J. Drug Delivery Sci. Technol.*, 2017, **41**, 157.
24 K. Moribe, M. Shibata, T. Furuishi, K. Higashi, K. Tomono and K. Yamamoto, *Chem. Pharm. Bull.*, 2010, **58**, 1096.
25 Z. M. Adib, S. Ghanbarzadeh, M. Kouhsoltani, A. Y. Khosroshahi and H. Hamishehkar, *Adv. Pharm. Bull.*, 2016, **6**, 31.
26 X. Liu, B. Shen, C. Shen, R. Zhong, X. Wang and H. Yuan, *J. Drug Delivery Sci. Technol.*, 2018, **45**, 367.
27 T. C. Laurent, U. B. G. Laurent and J. R. E. Fraser, *Ann. Rheum. Dis.*, 1995, **54**, 429.
28 M. Larsson and J. Duffy, *Annu. Trans. - Nord. Rheol. Soc.*, 2015, **23**, 27.
29 A. Dodero, R. Williams, S. Gagliardi, S. Vicini, M. Alloisio and M. Castellano, *Carbohydr. Polym.*, 2019, **203**, 349.
30 M.-A. Bolzinger, S. Briançon, J. Pelletier and Y. Chevalier, *Curr. Opin. Colloid Interface Sci.*, 2012, **17**, 156.
31 H. Todo, Y. Hasegawa, A. Okada, S. Itakura and K. Sugibayashi, *Chem. Pharm. Bull.*, 2021, **69**, 727.
32 E. R. Osorio-Blanco, F. Rancan, A. Klossek, J. H. Nissen, L. Hoffmann, J. Bergueiro, S. Riedel, A. Vogt, E. Rühl and M. Calderón, *ACS Appl. Mater. Interfaces*, 2020, **12**, 30136.

Received: 17th March 2023; Com. 23/7124